Cell Reports, Volume *36*

Supplemental information

Compartmentalization-aided interaction screening reveals extensive high-order complexes within the SARS-CoV-2 proteome

Weifan Xu, Gaofeng Pei, Hongrui Liu, Xiaohui Ju, Jing Wang, Qiang Ding, and Pilong Li

Supplemental Figure 1

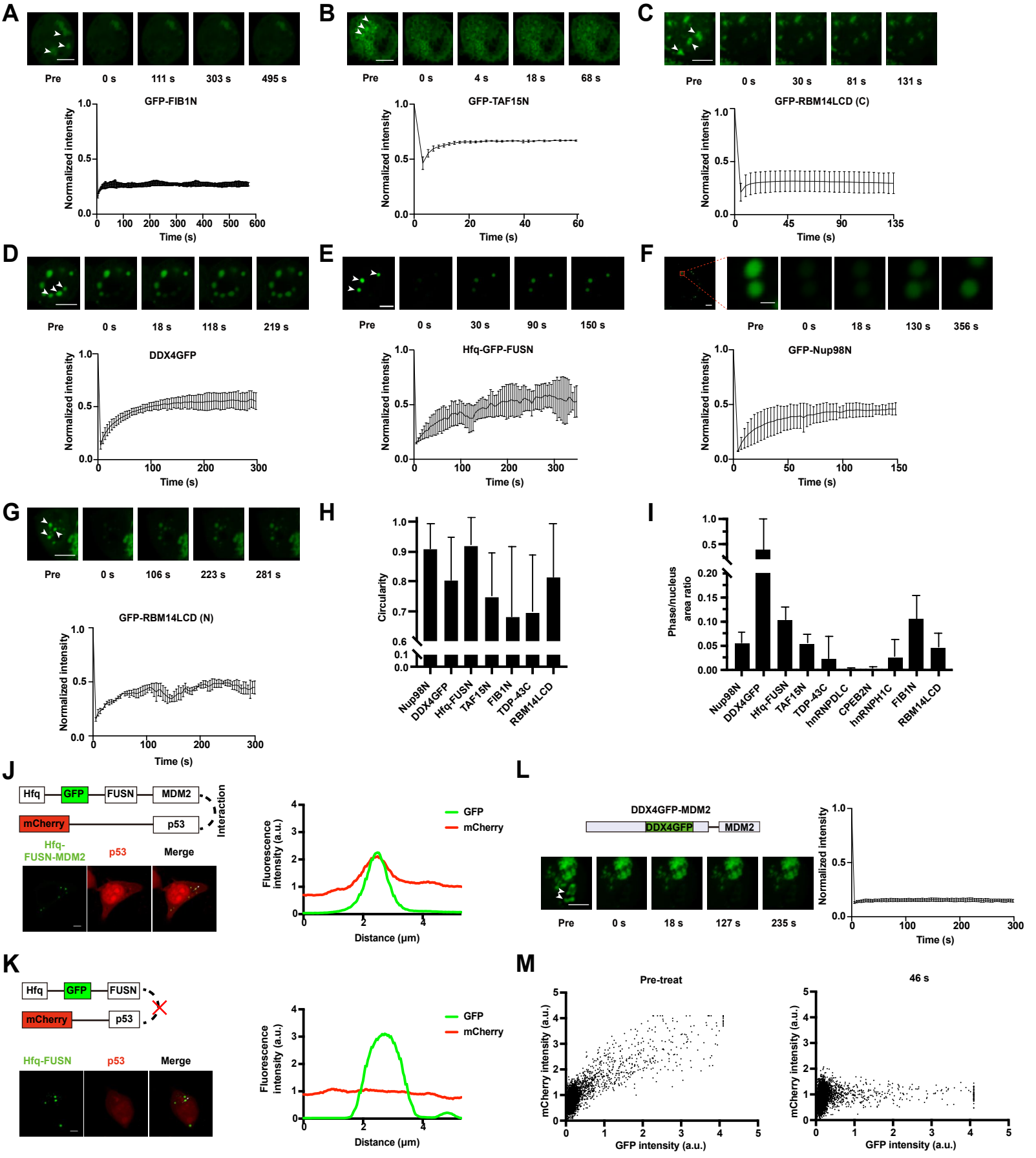

FigureS1. Characterization of scaffold candidates compartmentalizing and validating the direct interaction between p53 and MDM2 (Related to Figure1)

(A-G) FRAP analysis of scaffold candidates fused with GFP-tag in HEK293 cells. Scale bar, 5 μm. All assays were performed in triplicates.

(H) Histogram of the circularity of compartments formed by testing seven protein scaffolds in cells. n (Nup98N) = 100; n (DDX4GFP) = 182; n (FUSN) = 73; n (TAF15N) = 179; n (FIB1N) = 58; n (TDP-43C) = 60; n (RBM14LCD (N)) = 120. Each data point was determined by three independent assays, and error bars represent standard deviations. Values are means ± standard deviation.

(I) Histogram of the area ratio of phase-separated puncta to the nucleus, indicating the phase separation capability of the testing scaffolds. n = 6. Each data point was determined by three independent assays, and error bars represent standard deviations. Values are means ± standard deviation.

(J) FRAP analysis of DDX4GFP-MDM2 in HEK293 cells. Scale bars, 5 μm. All assays were performed in triplicates.

(K and L) Validation of the direct interaction between Hfq-GFP-FUSN-MDM2 and mCherry-p53 using CoPIC. The p53 fusion protein, as indicated by the mCherry signal, was recruited to the green compartment of Hfq-GFP-FUSN-MDM2 by the specific interaction (K). The co-expression of Hfq-GFP-FUSN and mCherry-p53 served as the control (L). Scale bars, 5 μm. All assays were performed in triplicates.

(M) Plots of Pearson’ s correlation coefficient for the intensity of and mCherry-p53 versus GFP-Nup98N-MDM2 pre-treatment and after 46 s. Each data point was determined by three independent assays.

Supplemental Figure 2

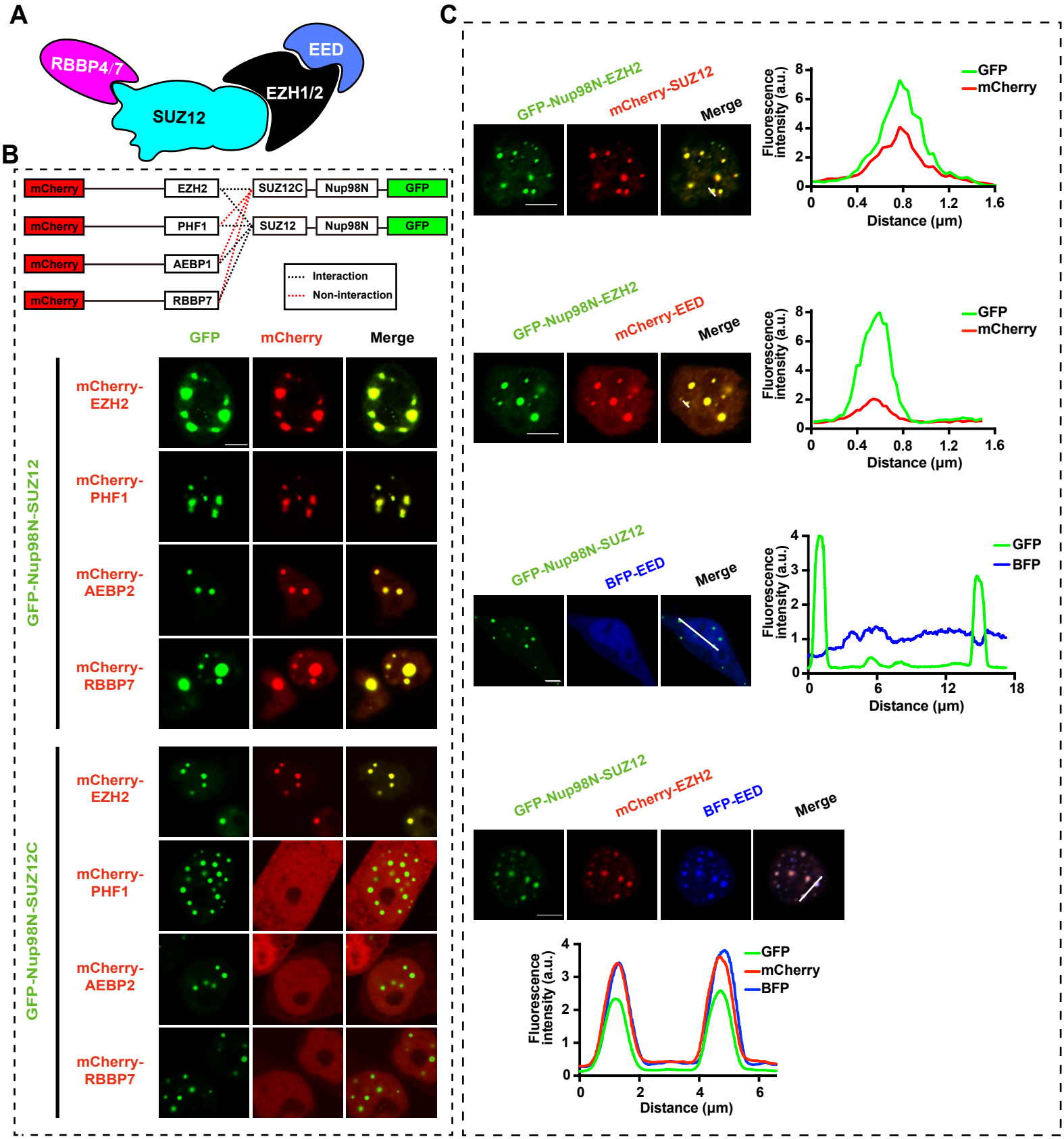

Figure S2. CoPIC analysis of the interaction patterns of SUZ12 with the binding factors and EZH2-mediated indirect interaction of SUZ12 with EED (Related to Figure 2)

(A) Schematic diagram depicting the architecture of the PRC2 complex.

(B) CoPIC analysis of pair-wise interactions between GFP-Nup98N fused SUZ12 (full-length SUZ12) or SUZ12C (C-terminal region of SUZ12) and mCherry-fused binding factors (EZH2, RBBP7, PHF1 and AEBP2). Scale bar, 5 μm. All assays were performed in triplicates.

(C) CoPIC analysis of the indirect interaction of SUZ12 with EED mediated by EZH2. Scale bars, 5 μm. All assays were performed in triplicates.

Supplemental Figure 3

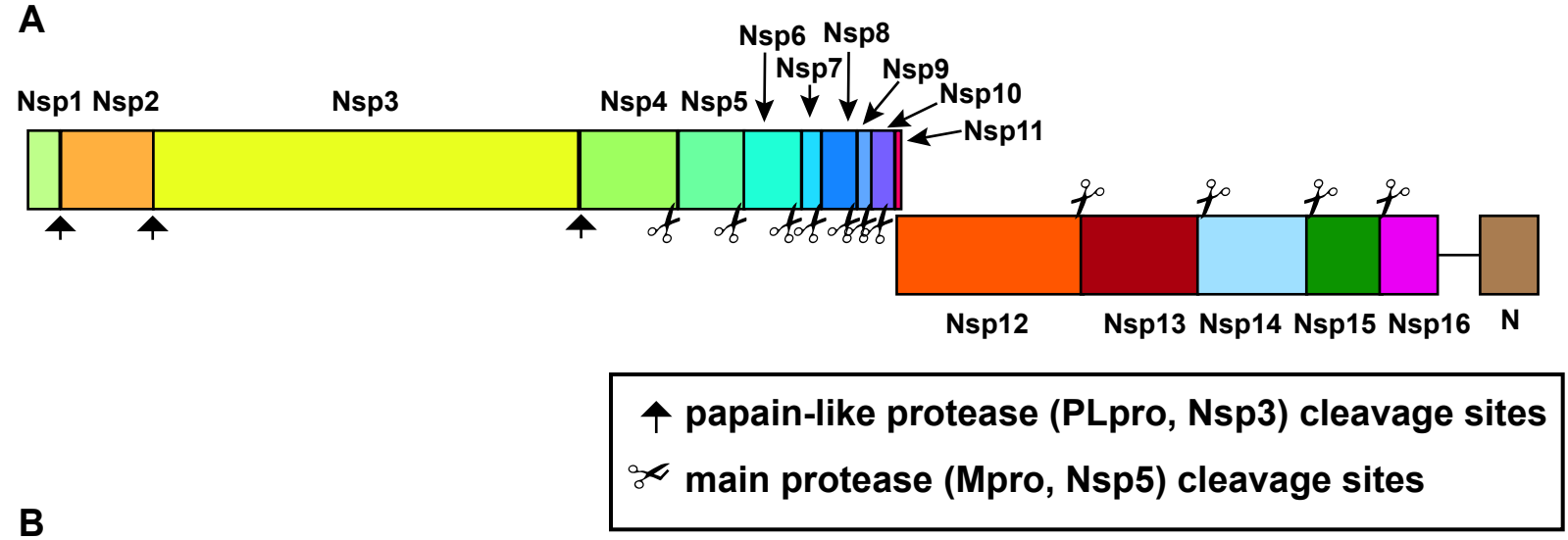

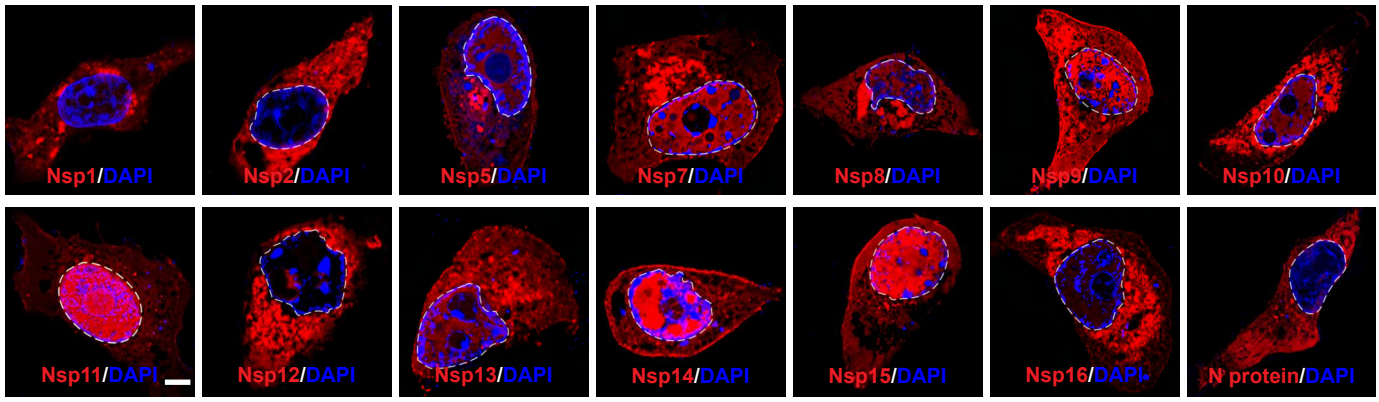

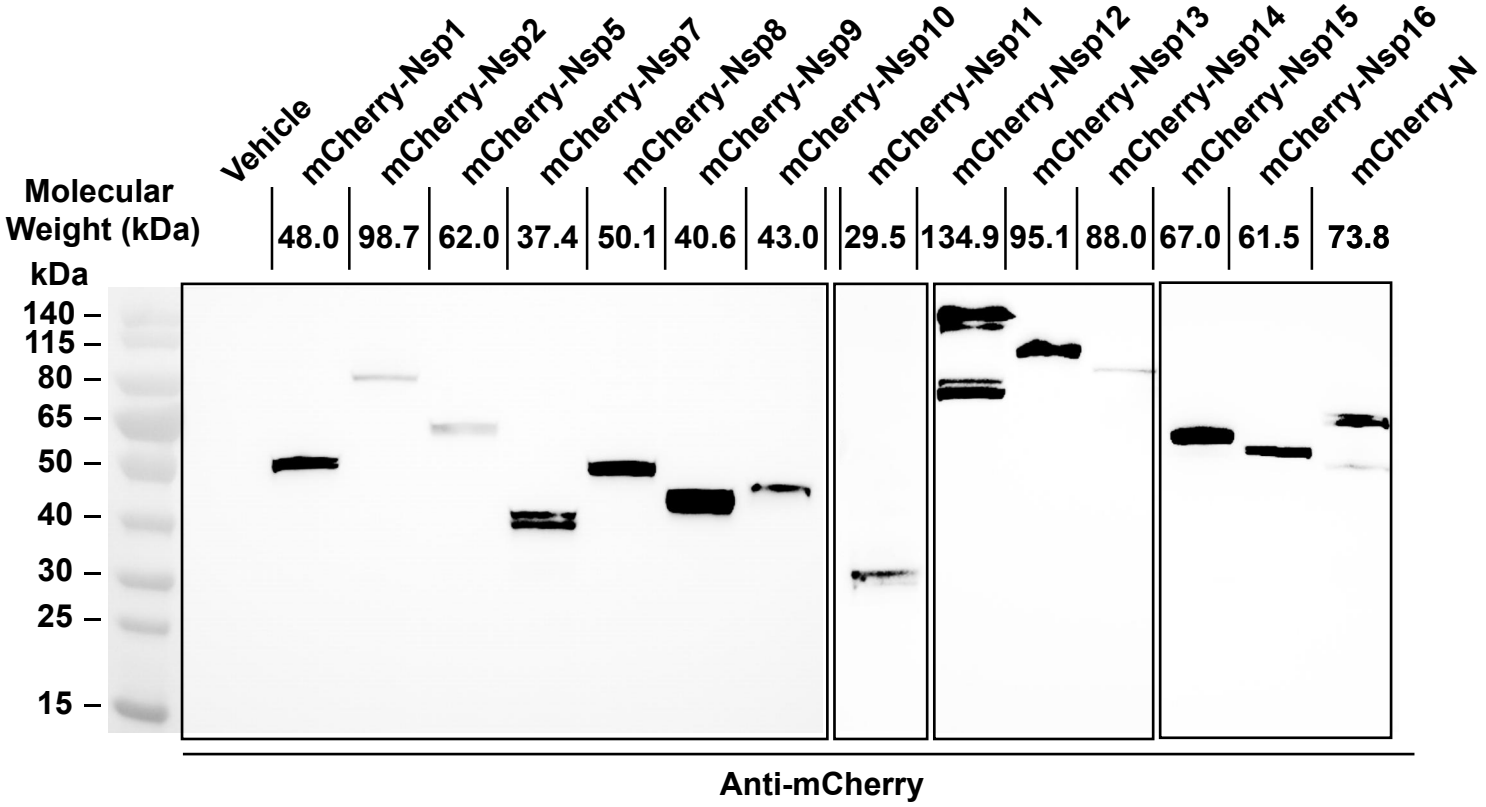

Figure S3. Genome annotation and subcellular localization of SARS-CoV-2 RTC-related factors (Related to Table 1 and Figure 3)

(A) SARS-CoV-2 genome annotation on replication/transcription-related factors.

(B) Subcellular localization of SARS-CoV-2 Nsps and N protein used in CoPIC screening. Scale bar, 5 μm.

(C) Western blot validation of the constructs fused with an mCherry tag expressed in Vero E6 cells. The cell lysates were extracted and examined with the specific antibody against mCherry.

Supplemental Figure 4

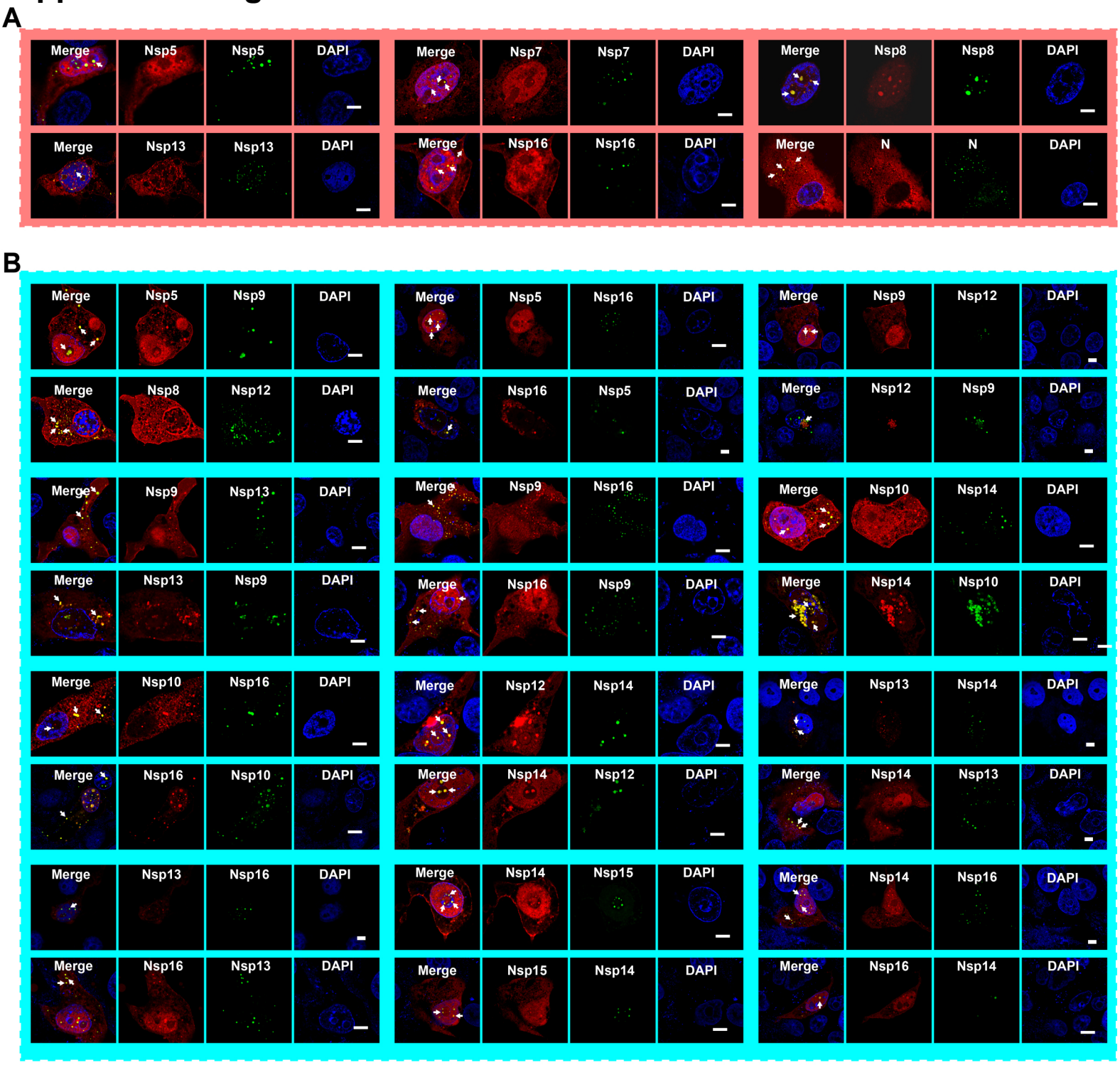

Figure S4. Positive pairwise (self- and bidirectional-) interactions of SARS-CoV-2 identified by CoPIC screening (Related to Figures 3, 4 and 5)

(A) Collections of positive self-interactions identified by CoPIC screening. All assays were performed in triplicates.Scale bar, 5 μm.

(B) Collections of positive bidirectional interactions identified by CoPIC screening. All assays were performed in triplicates.Scale bar, 5 μm.

Supplemental Figure 5

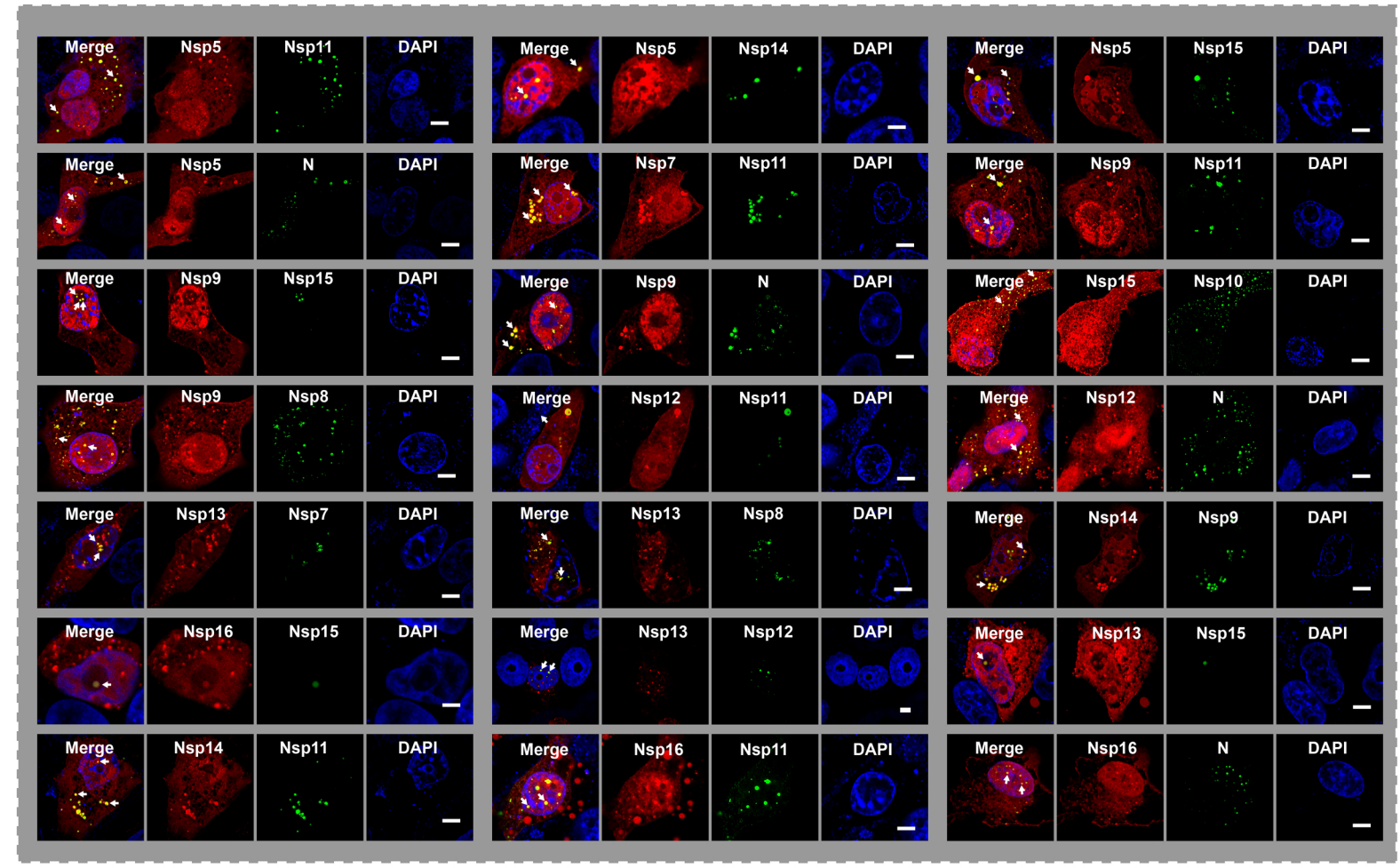

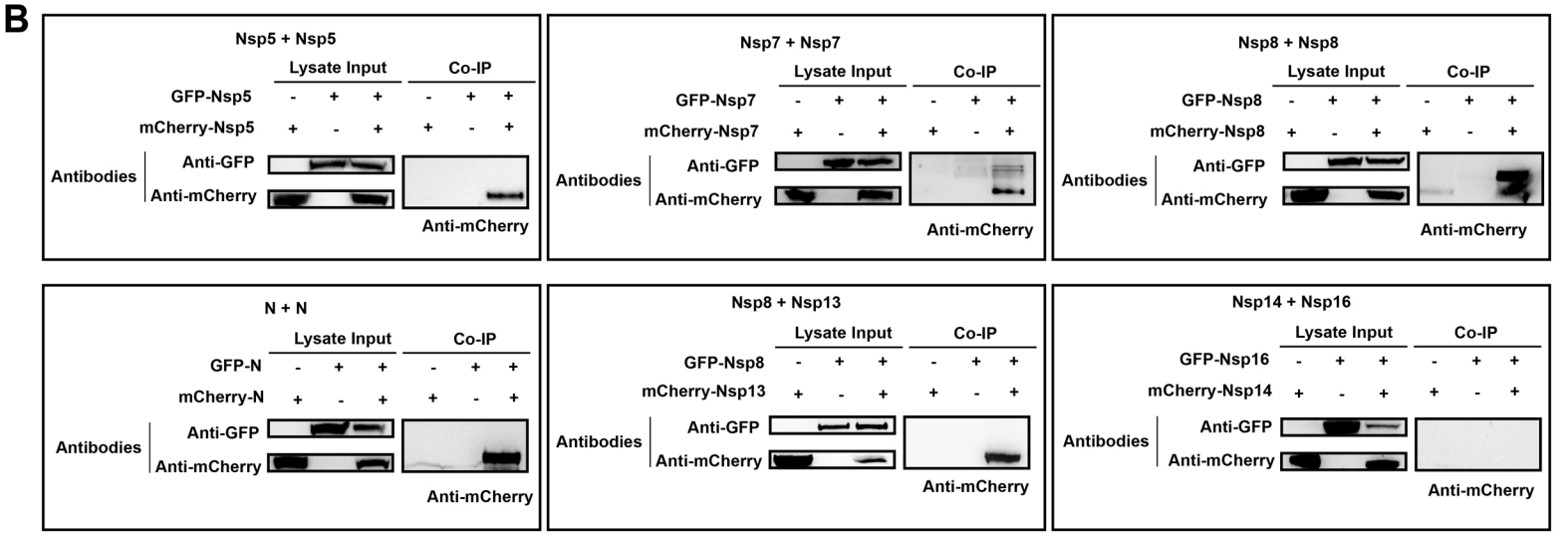

Figure S5. Positive pairwise (unidirectional-) interactions of SARS-CoV-2 identified by CoPIC screening (Related to Figures 3, 4 and 5)

(A) Collections of positive unidirectional interactions identified by CoPIC screening. All assays were performed in triplicates.Scale bar, 5 μm.

(B) Co-IP analysis of selected pairwise interactions identified by CoPIC screening.

Supplemental Figure 6

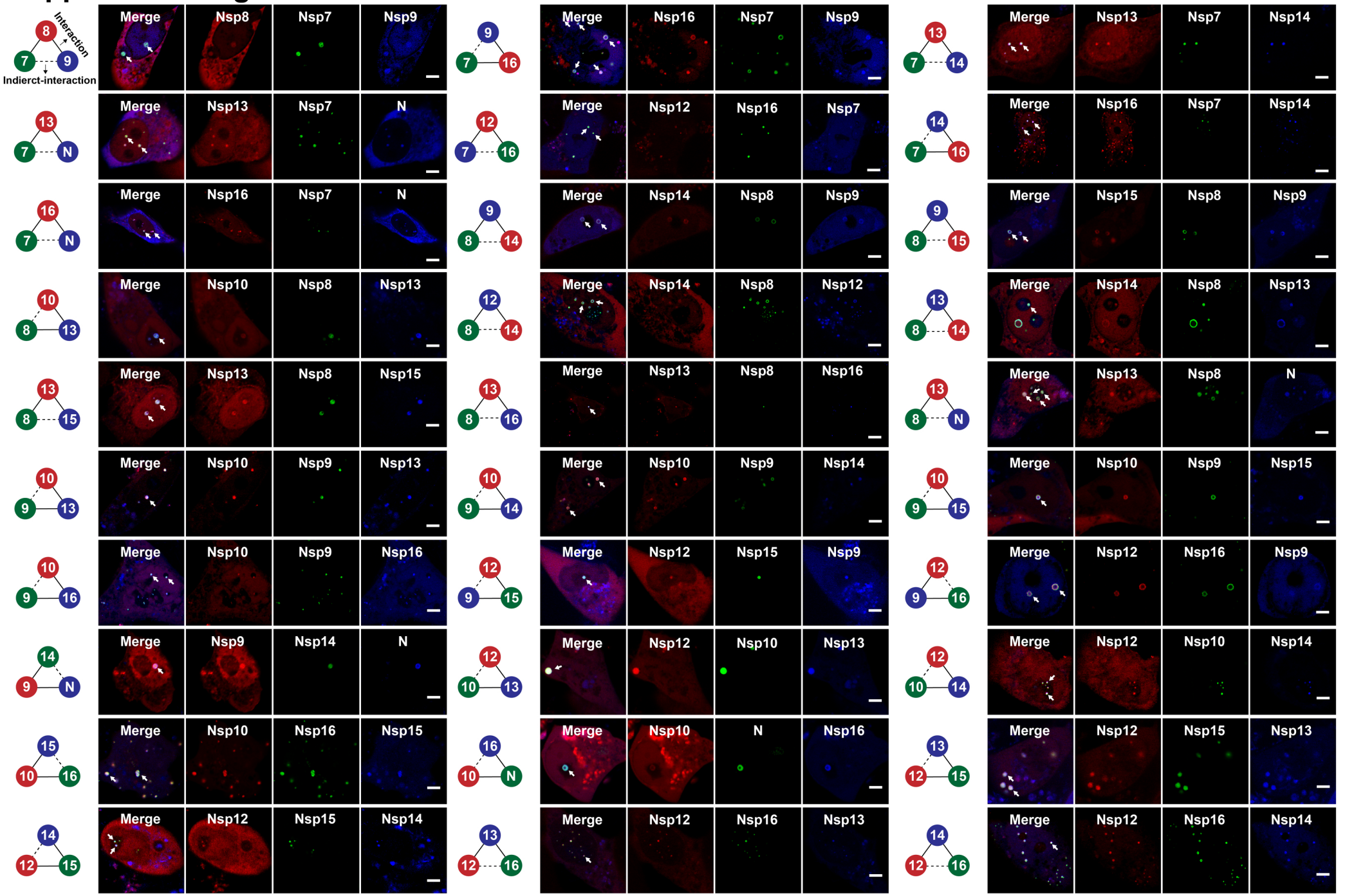

Figure S6. Collections of positive tertiary complexes identified by CoPIC screening (Related to Figure 6)

Positive tertiary interactions identified by CoPIC screening. All assays were performed in triplicates. Scale bar, 5 μm.

Supplemental Figure 7

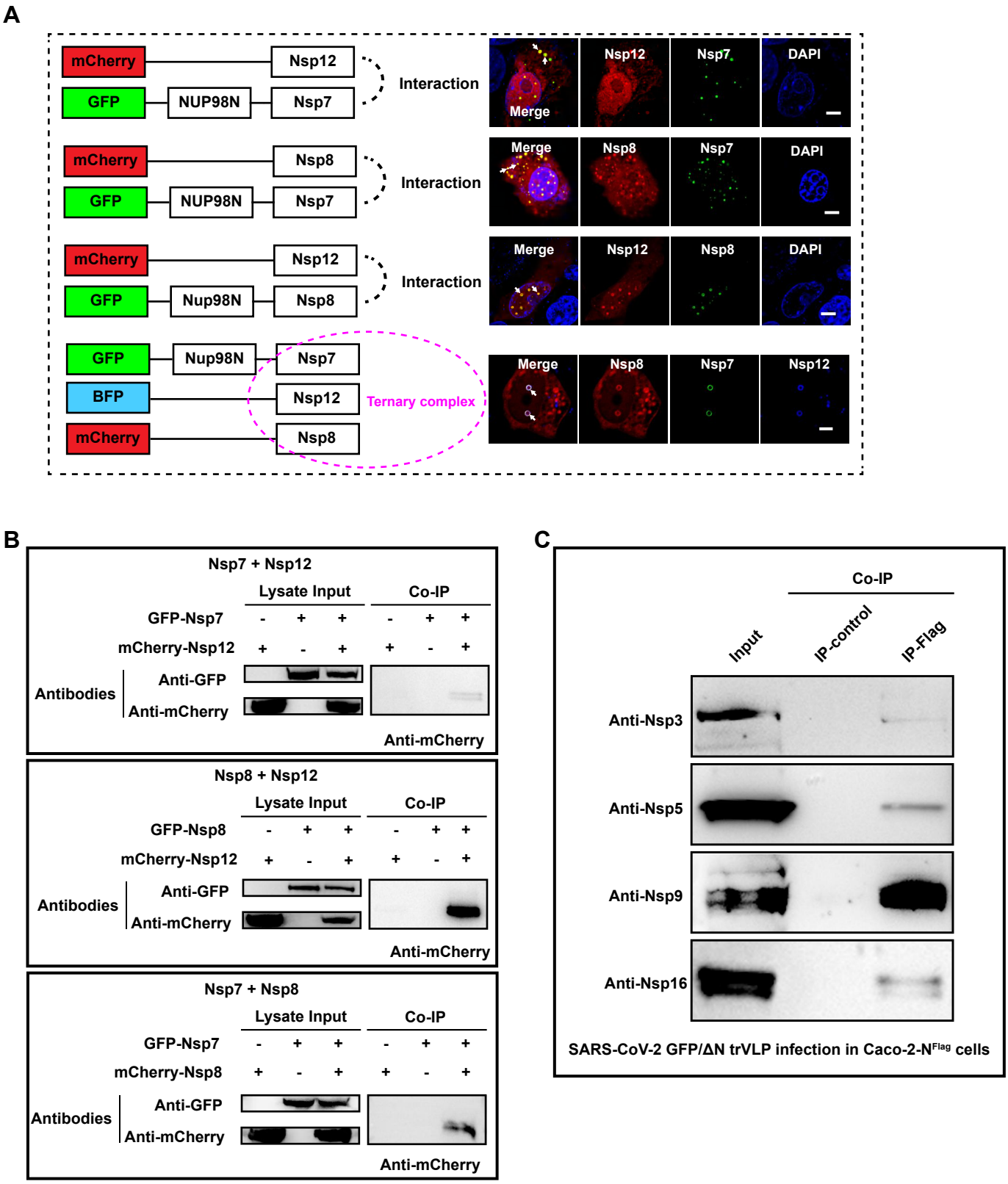

Figure S7. Characterization of mutual interactions among Nsp7, Nsp8, and Nsp12 (Related to Figure 6)

(A) CoPIC analysis of binary and tertiary interactions among Nsp7, Nsp8, and NSp12. All assays were performed in triplicates.Scale bar, 5 μm.

(B) CoIP validation of pairwise interactions between Nsp7 and Nsp8, Nsp7 and Nsp12, Nsp8 and Nsp12. All assays were performed in triplicates.

(C) CoIP analysis of Nprotein and binding candidates under SARS-CoV-2 GFP/ΔN trVLP infection in Caco-2-N^{Flag} cells.

Supplemental Figure 8

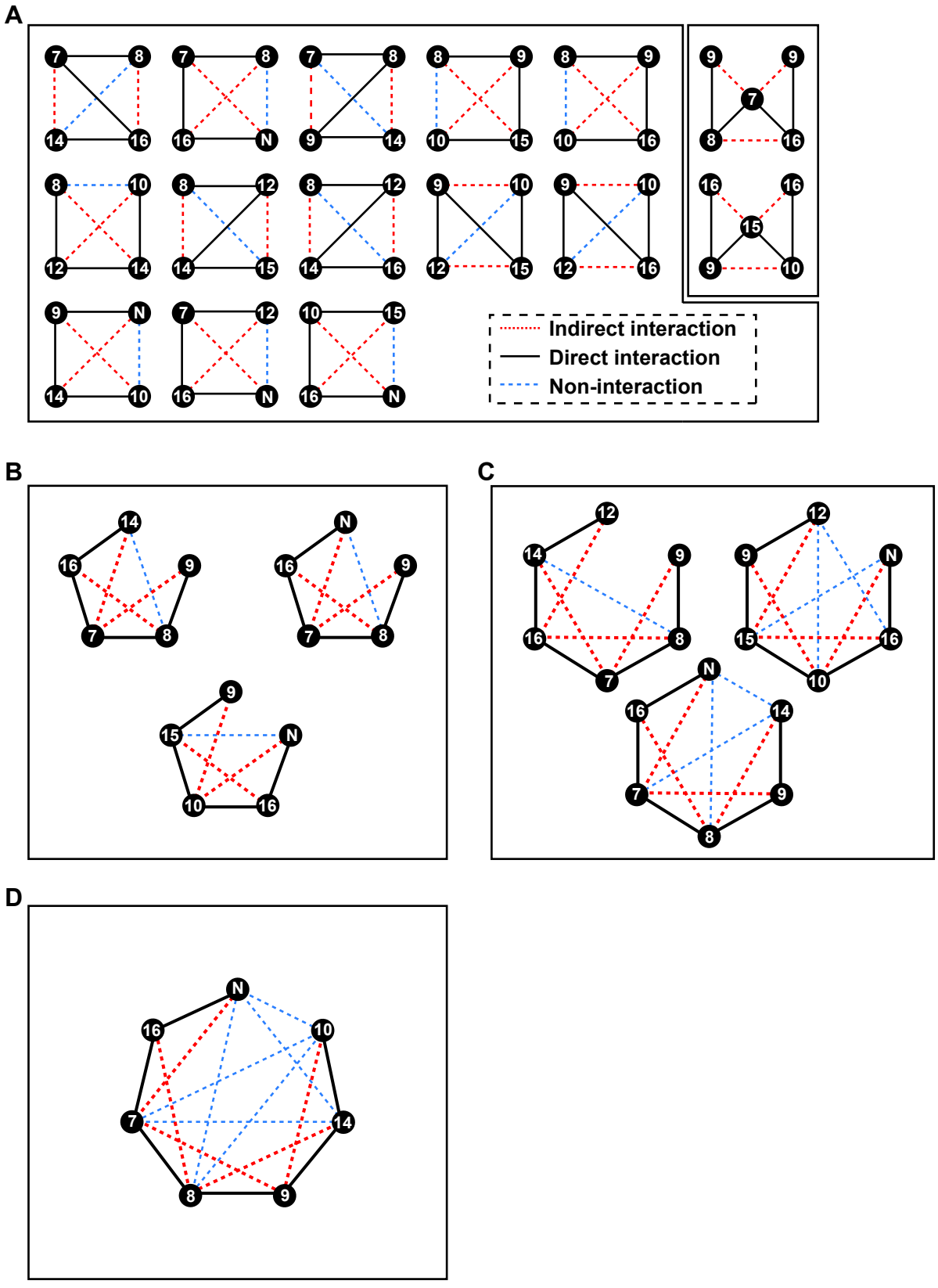

Figure S8. Higher-order complexes deduced from CoPIC analysis (Related to Figure 7)

(A) List of quaternary complexes deduced from CoPIC analysis.

(B) List of quinary complexes deduced from CoPIC analysis.

(C) List of six-membered complexes deduced from CoPIC analysis.

(D) List of seven-membered complexes deduced from CoPIC analysis.

Table S1 Sequence information for RTC-related viral proteins of SARS-CoV-2 used in the study for plasmid construction. (Related to Figure 3)

Protein	Accession Number	Nucleotide positions	Position in polyprotein	Protein length (aa)
Nsp1	YP_009725297.1	266-805	M1-G180	180
Nsp2	YP_009725298.1	806-2719	A181-G818	638
Nsp5	YP_009725301.1	10055-10972	S3264-Q3569	306
Nsp7	YP_009725303.1	11843-12091	S3860-Q3942	83
Nsp8	YP_009725304.1	12092-12685	A3943-Q4140	198
Nsp9	YP_009725305.1	12686-13024	N4141-Q4253	113
Nsp10	YP_009725306.1	13025-13441	A4254-Q4392	139
Nsp11	YP_009725312.1	13442-13480	S4393-V4405	13
Nsp12	YP_009725307.1	12480-16236	V4406-Q5324	919
Nsp13	YP_009725308.1	16237-18039	A5325-Q5925	601
Nsp14	YP_009725309.1	18040-19620	A5926-6452	527
Nsp15	YP_009725310.1	19621-20658	S6453-Q6798	346
Nsp16	YP_009725311.1	20659-21555	S6799-N7096	298
N protein	YP_009724397.2	28274-29533	--	419

Table S2 Collections of reported interaction patterns of SARS-CoV. (Related to Figure 4)

Number	Positive interactions	References
1	Nsp2-Nsp2	(von Brunn et al., 2007)
2	Nsp2-Nsp7	(Pan et al., 2008)
3	Nsp2-Nsp8	(von Brunn et al., 2007)
4	Nsp2-Nsp11	(von Brunn et al., 2007)
5	Nsp2-Nsp15	(Pan et al., 2008)
6	Nsp2-Nsp16	(von Brunn et al., 2007)
7	Nsp5-Nsp5	(von Brunn et al., 2007)
8	Nsp5-Nsp7	(von Brunn et al., 2007)
9	Nsp5-Nsp8	(von Brunn et al., 2007)
10	Nsp5-Nsp12	(Pan et al., 2008)
11	Nsp5-Nsp14	(Pan et al., 2008)
12	Nsp7-Nsp7	(von Brunn et al., 2007)
13	Nsp7-Nsp8	(von Brunn et al., 2007)
14	Nsp7-Nsp9	(von Brunn et al., 2007)
15	Nsp7-Nsp13	(von Brunn et al., 2007)
16	Nsp8-Nsp8	(von Brunn et al., 2007)
17	Nsp8-Nsp9	(von Brunn et al., 2007)
18	Nsp8-Nsp12	(von Brunn et al., 2007)
19	Nsp8-Nsp13	(von Brunn et al., 2007)
20	Nsp8-Nsp14	(von Brunn et al., 2007)
21	Nsp9-Nsp9	(Sutton et al., 2004)
22	Nsp10-Nsp10	(Su et al., 2006)
23	Nsp10-Nsp14	(Pan et al., 2008)
24	Nsp10-Nsp16	(Pan et al., 2008)
25	Nsp12-Nsp13	(von Brunn et al., 2007)
26	Nsp13-Nsp13	(von Brunn et al., 2007)
27	Nsp15-Nsp15	(Joseph et al., 2007)
28	N protein-N protein	(Chen et al., 2007)